

A new approach towards the Debye length challenge for specific and label-free biological sensing based on field-effect transistors

Ie Mei Bhattacharyya¹, Izhar Ron¹, Ankit Chauhan¹, Evgeny Pikhay², Doron Greental², Niv Mizrahi², Yakov Roizin², Gil Shalev^{1,3*}

¹ School of Electrical Engineering, Ben-Gurion University of the Negev, Israel

² Tower Semiconductor, PO Box 619, Migdal Haemek, Israel

³ The Ilse-Katz Institute for Nanoscale Science and Technology, Ben-Gurion University of the Negev, POB 653, Beer-Sheva 8410501, Israel

*corresponding author: gshalev@bgu.ac.il.

SI§1 – APTMS surface characterization

Characterization of APTMS monolayers by spectroscopic ellipsometry

To optically evaluate the thickness of the APTMS layer, J.A. Woollam Alpha-SE Ellipsometer was used to carry out spectroscopic ellipsometry of the samples before and after silanization. Figure 1a shows the layer structure that was used for modeling and the raw data (psi and delta values).

Three different spots on the same sample were measured assuming an initial native oxide thickness of 19-20 Å. The thickness of both the oxide and the APTMS layer were fitted. The results of the fitting are shown in Figure 1b. We observe the fit result of the oxide is close to the estimated value. The average of the APTMS layer thickness is 23 Å which probably indicates the formation of a multilayer and is not significantly higher than the expected thickness for a monolayer (~5 Å chain length, assuming 1 Å per bond). This trend is in good agreement with previous studies of amino-silane layers on SiO₂.^[1]

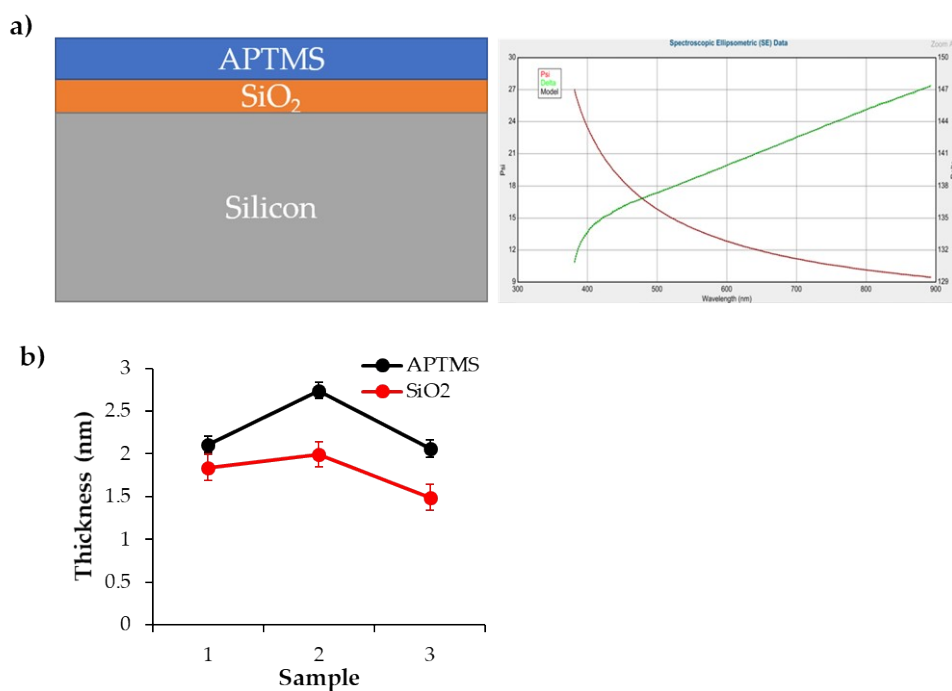


Figure 1. a) Layer structure of the sample used for modeling ellipsometry measurements (left) and raw data (right). **b)** Thickness of each layer measured using ellipsometry on three different samples.

Characterization of APTMS monolayers by atomic force microscopy (AFM)

Surface topography of the samples was characterized by Atomic force microscopy (AFM) in order to evaluate APTMS layer roughness as a measure of layer quality and uniformity (Multiview 4000, Nanonics Imaging Inc.). AFM images for bare SiO₂ and APTMS modified samples before and after hydrolysis are shown in Figure 2a. Root mean square (RMS) surface roughness and roughness average of the three samples are presented in Figure 2b.

The roughness information is extracted from AFM imaging to determine the quality of the APTMS organic layer on top of the Si/SiO₂ substrate. The measured RMS roughness of the bare SiO₂ is of the order of 3-4 Å, which indicates that it is a smooth surface and is in agreement with previously reported values.^[2] However, the addition of the APTMS layer increases the roughness for both non-hydrolyzed and hydrolyzed layers. In both cases, the increase in roughness is small compared to the measured thickness of the layers which indicates that a relatively dense layer, mostly free of large oligomeric and polymeric forms of the silane molecule, which would otherwise result in a much rougher surface.

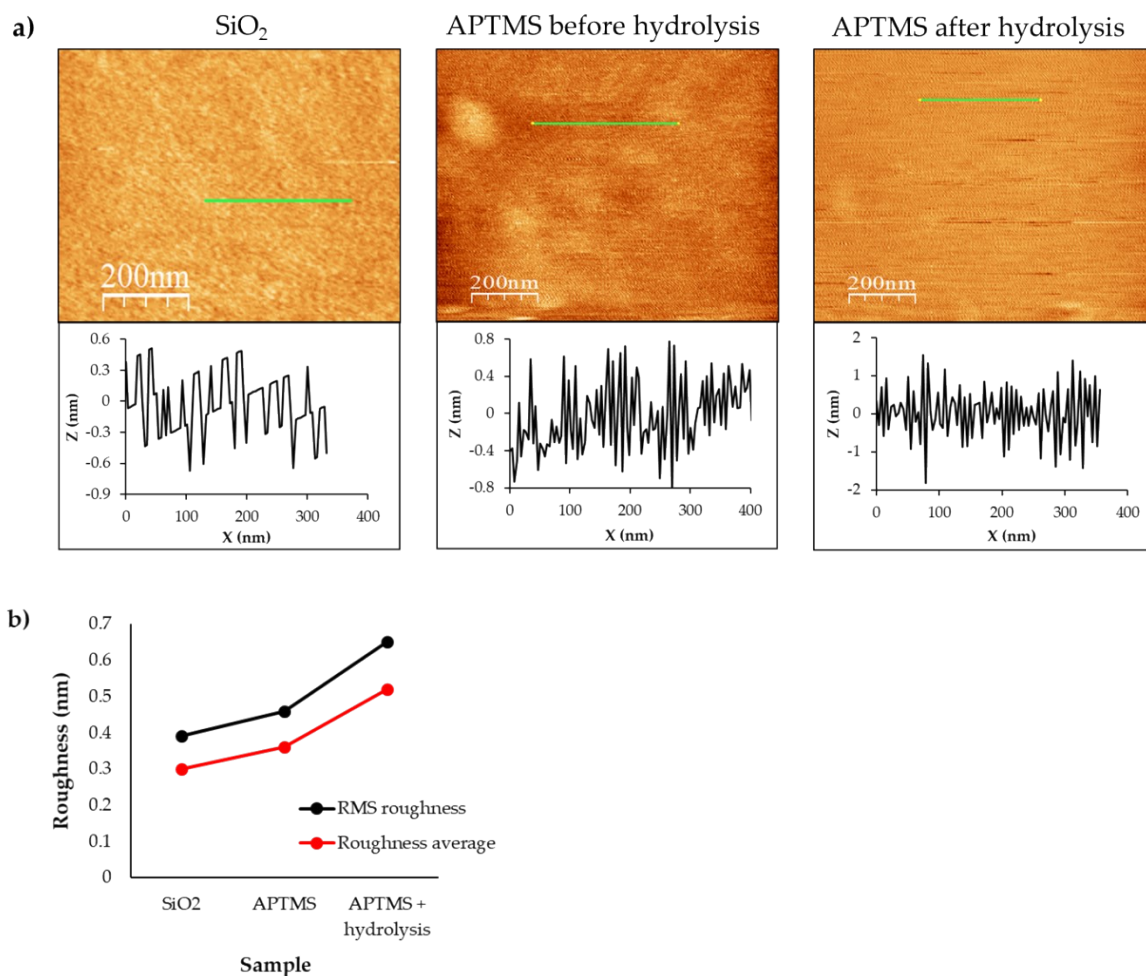


Figure 2. a) AFM images of bare SiO₂ surface (left), APTMS layer before (middle) and after (right) hydrolysis. **b)** RMS roughness values extracted from AFM imaging of bare SiO₂, APTMS and APTMS with hydrolysis samples.

Characterization of APTMS monolayers by electrochemical impedance spectroscopy (EIS)

Electrochemical impedance spectroscopy (EIS) was used for the surface characterization of the bare SiO₂ and APTMS modified surfaces. To avoid the various capacitances associated with the substrate, all EIS measurements were performed on degenerately doped Si wafer. In this experiment, the sample was placed in a three-electrode electrochemical cell in 10 mM phosphate buffer saline (PBS) buffer, pH 7.4. The working electrode was made by contacting the sample from the back using conductive carbon paint spread on the scratched back face of the substrate. Pt wire was used as counter electrode and Ag/AgCl electrode (ALS-Japan) was used as the reference electrode. The measurement was carried out using a PalmSens4 potentiostat (PalmSens, The Netherlands) in a frequency scan mode, where a small AC signal

of 10mV was applied in the frequency range between 0.1 Hz and 100kHz. The impedance, Z (real and imaginary parts) was recorded throughout this range. The C'' vs C' Nyquist plots measured for oxide and APTMS-modified samples are presented in Figure 3, together with a scheme of the experimental setup. The selected equivalent electrical circuit is shown in Figure 4.

In this circuit, the oxide layer is represented by an RC (C_2 , R_2) circuit, and the molecular APTMS layer, in combination with the interface between the oxide and the electrolyte (where an electrical double layer is formed), is represented by a capacitor, C_1 – the double layer capacitance, in parallel with a Warburg impedance component (W_1), assigned to diffusion processes of ions to the interface. A constant phase element (Q_1) is added in series to correct for monolayer imperfections and inhomogeneities, and finally in series a resistor representing the solution (electrolyte) resistance is added (R_1). Only the circuit components used to model the double layer, i.e. double layer capacitance C_1 and the Warburg impedance W_1 change upon the formation of a molecular layer at the interface. The fitted values for C_1 and W_1 for both the oxide and APTMS modified samples are presented in Table 1.

Table 1 shows the capacitive change in C_1 of more than an order of magnitude upon addition of the APTMS layer as compared to that in the case of the oxide sample. The reduction in double layer capacitance with the addition of the APTMS molecular layer on top of the oxide can be attributed to a thicker layer of counter ions attracted towards the interface due to the addition of positive charges resulting in a smaller capacitor. These results are in good agreement with previous studies on similar electrolyte-insulator-semiconductor (EIS) silicon-based systems.^[3]

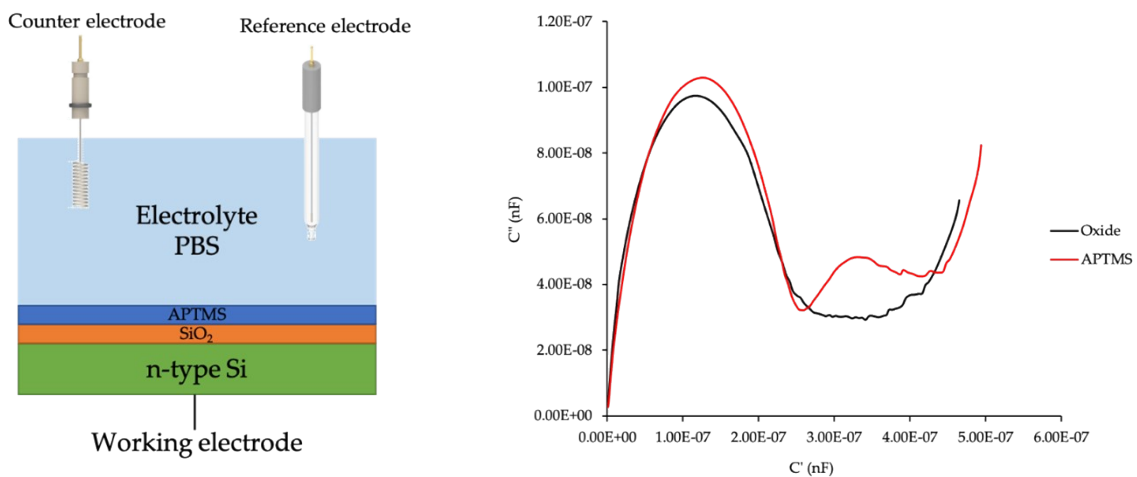


Figure 3. Experimental setup (left) and Nyquist plot of EIS data (right)

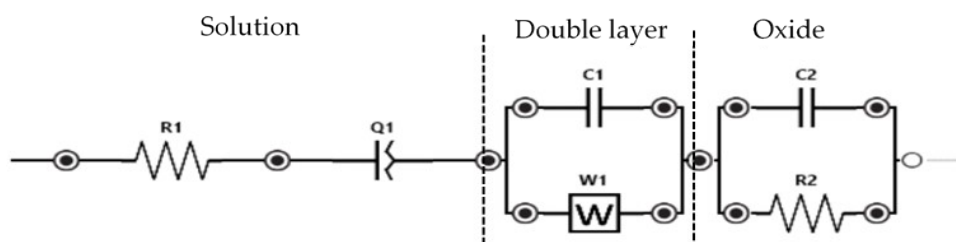


Figure 4. Equivalent electrical circuit used for fitting of EIS data

Table 1. Fitted values of the double layer capacitance C1 and the Warburg impedance W1

Sample	Buffer	C1 (nF)	W1 (k σ)
Bare	10mM PBS	5636	0.17
APTMS		536.3	245.9

SI§2 – Immobilization of antiPSA and surface characterization

Synthetic route for the immobilization of antiPSA bio-receptor layer

APTMS-terminated layers were modified with glutaraldehyde (GA) crosslinker, which serves to anchor the antiPSA antibodies. The surfaces were immersed in 0.5% aqueous solution of GA for one hour, to achieve an aldehyde-terminated surface. The samples were then immersed in 1 μ g/ml solution of antiPSA, produced in rabbit, in 0.1 mM PBS, pH 7.4 overnight. This strategy is based on the common knowledge that antibodies are commonly immobilized to aldehyde-terminated surfaces based on the reaction between amine moieties of the antibody and the aldehyde group^[4].

Characterization of antiPSA monolayers by ellipsometry

For the optical evaluation of the thickness of the antiPSA layer immobilized on the APTMS-modified samples, spectroscopic ellipsometry was carried out in a similar manner as described above for the chemical modifications. The model used for the fit and the results are shown in Figure 5.

This calculated thickness can be interpreted as: for IgG layers (where the long physical dimension is 14 nm), models have been developed where the saturation effective thickness was 5 nm.^[5] This saturation thickness was evaluated for immobilization concentrations 100 times higher than what is used here (10 μ g/ml), hence it may be considered an expected effective thickness.

Anti-PSA		Sample	Layer thickness
APTMS		APTMS	$0.73 \pm 0.06\text{nm}$
SiO ₂		AntiPSA	$2.34 \pm 5.64 \text{ nm}$
p-type Si (500 μm)			

Figure 5. Ellipsometry model and fit values for antiPSA modified samples.

Characterization of antiPSA monolayers by AFM

Surface topographic characterization of the antiPSA layer was carried out in a similar manner as for the former layer construction steps. AFM images are shown in Figure 6 and calculated surface roughness values are shown in Table 2.

Antibody height in AFM is typically in the range of 4-6.5 nm^[6] and the cross section of the antiPSA surface shown for the APTMS-toluene substrate may indicate an antibody in good agreement with the typical imaged dimensions. The lack of such features in the APTMS-methanol substrate cannot rule out the presence of antibodies in other areas of the samples, as clearly indicated from ellipsometry characterization and roughness analysis. As for the roughness, this value may not provide direct interpretation of the layer quality, but clearly it is far higher than the roughness of the underlying substrates, which clearly suggests the addition of a partial layer of much larger molecules, and this was shown before even for less smooth substrates than in this current work.^[7]

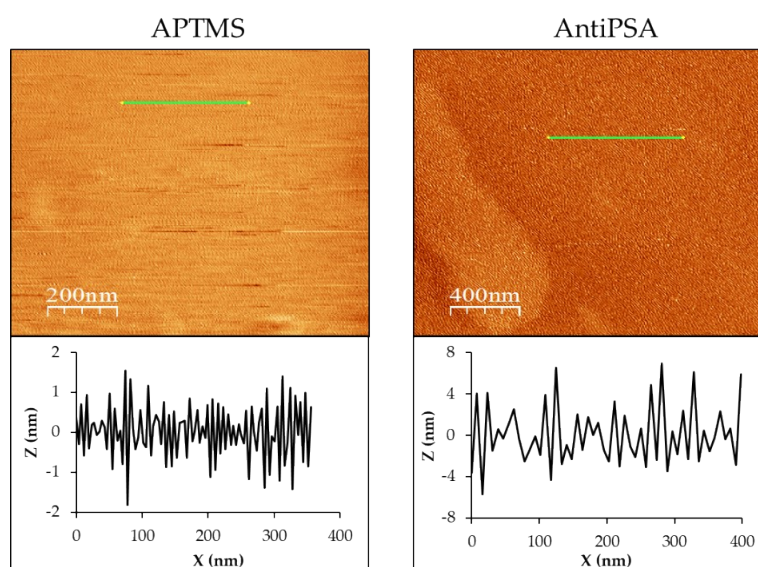


Figure 6. Comparison of the AFM images of APTMS modified samples and antiPSA modified samples.

Table 2. Roughness values extracted from the AFM images of the APTMS and antiPSA modified samples

Sample	RMS roughness (nm)	Roughness average (nm)
APTMS	0.65	0.52
AntiPSA	2.72	2.26

Characterization of antiPSA monolayers by EIS

EIS analysis was performed as described in detail above (as before, all EIS measurements were performed on a degenerately doped silicon wafer to avoid with the various capacitances associated with the wafer). The imaginary vs. real capacitance Nyquist plot, the equivalent electrical circuit used to model the resulting layers and the fitted values are shown in Figure 7. Figure 7a shows a pronounced difference in the ratio of the imaginary and real parts of the capacitance in the low frequency regime between APTMS, GA and anti-PSA modified samples. In the equivalent circuit used for model fitting, the oxide layer and the molecular APTMS layer are both combined with the interface between the solid and the electrolyte (where an electrical double layer is formed), and are represented by a capacitor (C3). Also shown is the double layer capacitance (C2), in parallel with a Warburg impedance component (W1), assigned to diffusion processes of ions to the interface. A constant phase element (Q1) is added in series to correct for monolayer imperfections and inhomogeneities, and finally in series a resistor representing the solution (electrolyte) resistance is added (R1). Here, the double layer and antiPSA are considered as separate layers because they are very different in terms of the size of the molecules comprising them. Therefore, the analysis output gives two important values – the double layer capacitance C2 and the bioreceptor (antiPSA) layer capacitance C1. It can be seen from the table in Figure 7b that the double layer capacitance C2 slightly decreases after the addition of GA on the APTMS samples. However, in the case of antiPSA-immobilized samples, we observe that C2 does not change compared to that in the GA-modified samples and the need to introduce an additional RC parallel network to obtain the best fit to the measured plot confirms the presence of a diffuse layer of antiPSA molecules immobilized on the surface since $C2 > C1$.

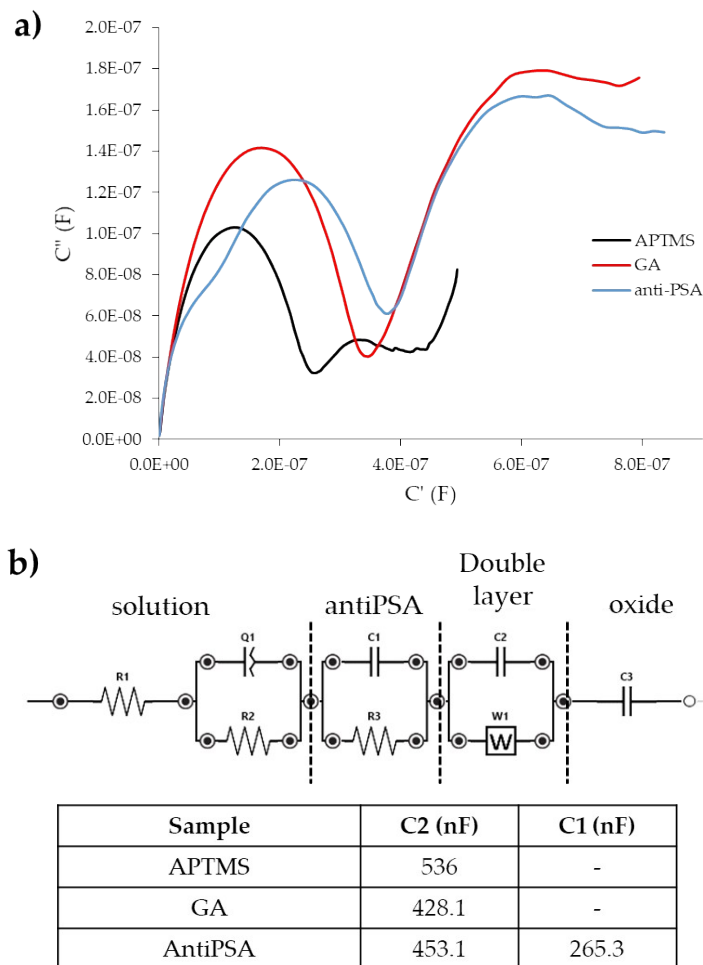


Figure 7. a) C'' vs C' plot for APTMS, GA and antiPSA modified samples. **b)** Equivalent circuit and the fitted parameters.

References

- [1] M. Zhu, M. Z. Lerum, W. Chen, *Langmuir* **2012**, DOI 10.1021/la203638g.
- [2] I. Ron, L. Sepunaru, S. Ltzhakov, T. Belenkova, N. Friedman, I. Pecht, M. Sheves, D. Cahen, *J. Am. Chem. Soc.* **2010**, DOI 10.1021/ja907328r.
- [3] H. Einati, A. Mottel, A. Inberg, Y. Shacham-Diamanda, *Electrochim. Acta* **2009**, *54*, 6063.
- [4] Z. H. Wang, G. Jin, *Colloids Surfaces B Biointerfaces* **2004**, DOI 10.1016/j.colsurfb.2003.12.012.
- [5] D. S. Wang, C. C. Chang, S. C. Shih, C. W. Lin, *Biomed. Eng. - Appl. Basis Commun.* **2009**, DOI 10.4015/S1016237209001386.
- [6] M. L. Jeong, K. P. Hyun, Y. Jung, K. K. Jin, O. J. Sun, H. C. Bong, *Anal. Chem.* **2007**, DOI 10.1021/ac0619231.

- [7] V. Ierardi, F. Ferrera, E. Millo, G. Damonte, G. Filaci, U. Valbusa, in *J. Phys. Conf. Ser.*, **2013**.